Lithium Ion Battery

DOI: 10.1002/anie.201300896

Catalyst-free Direct Growth of a Single to a Few Layers of Graphene on a Germanium Nanowire for the Anode Material of a Lithium Battery**

Hyungki Kim, Yoonkook Son, Chibeom Park, Jaephil Cho, and Hee Cheul Choi**

Graphite is a representative anode material for Li secondary ion batteries. Although graphite is highly reliable in its performance, the intrinsically low specific capacity (372 $mA\,h\,g^{-1}$) limits its application to electronic devices of low-power consumption. Several semiconductor or metal elements that are known to form alloys with Li, such as Si,[1] Ge,[2] Sn,[3] and so forth, have been intensively studied as a replacement of graphite since the theoretical specific capacities of these materials are much higher than that of graphite, which is essential for high-power applications, such as electric vehicles. Recently, despite the low specific capacity (1600 $mA\,h\,g^{-1}$)[2] relative to that of Si (4200 $mA\,h\,g^{-1}$),[1] Ge nanowires (NWs) have attracted much interest because Ge has a higher electrical conductivity (10^4 times) and faster lithium ion diffusivity (400 times) than Si,[4,5] allowing the expectation for Ge to show a high performance as anode in a Li ion battery especially at high rates.

Similar to the case of Si, however, one critical issue of Ge regarding its use as anode is its large volume expansion of about 370% occurring during the lithiation/delithiation cycle.[2] The large strain induced by the expansion causes the pulverization of the electrode from the current collector, which results in a poor cycle life. A potential strategy to overcome the large volume expansion problem is to mechanically protect the Ge NWs by strong and electrically conducting components. For this purpose, carbon-based materials including amorphous carbon and reduced graphene oxide (RGO) have been examined. Especially, RGO is advantageous as it still employs intrinsic novel properties of graphene, such as a high electrical conductivity, mechanical stability, surface area, and chemical stability.[6–9] Most of the RGO composites have been prepared by mixing RGO and electrochemically active materials in solution phase[6,8] or by co-reduction of an electrochemically active material precursor and GO.[7,9] However, for such a bulk composite-type system it is difficult to provide a high-quality layer coating, which frequently results in poor capacity retention and short cycle life because of 1) inhomogeneity of RGO itself in its size and quality in terms of the degree of reduction, and 2) inhomogeneous miscibility of multiple components.

An ideal approach to protect Ge NWs from its volume expansion is to directly grow graphene on a Ge NW surface by chemical vapor deposition (CVD). This approach would guarantee not only mechanical tight holding of the Ge NWs but also high electrical conductivity over the electrode throughout long cell cycles. Herein, we report a metal-catalyst-free direct growth of a single to a few (less than four) layers of graphene on a Ge NW (Gr/Ge NW). The formation of a graphitic carbon layer on a Ge NW has been reported by several groups.[10–12] However, graphitic layers of these studies are very thick (more than ten layers). Moreover, the quality of the graphitic layer in terms of the degree of long-range order and defect level has not been clarified. Such a thick graphene coating on Ge NWs is not proper for Li ions to diffuse into and out of the Ge NWs. On the contrary, our Gr/Ge NW is composed of a single to a few layers of high-quality graphene as confirmed by high-resolution TEM (HRTEM) and Raman spectroscopy. The Gr/Ge NW also shows a high performance as anode in a Li ion battery as it exhibits a high reversible specific capacity of 1059 $mA\,h\,g^{-1}$ even after 200 cycles at a rate of 4.0 C (= 4.8 $A\,g^{-1}$) with a capacity retention of 90% during 200 cycles.

The Gr/Ge NW was synthesized by growing graphene on pre-synthesized individual Ge NWs by a metal-catalyst-free CVD process. The Ge NWs of an average diameter of 46 nm were synthesized by a vapor–liquid–solid (VLS) process at 760 °C employing $GeCl_4$ as a liquid Ge precursor as reported.[13] Figure 1a displays a representative scanning electron microscopy (SEM) image of as-grown Ge NWs, showing a high yield of homogenous Ge NWs. A HRTEM image of an as-grown Ge NW shows the single crystalline lattice of a Ge NW with an about 4 nm thick native GeO_x layer (Figure 1b). The CVD process was then used for the growth of graphene layers directly on a Ge NW using the same reactor used for the growth of a Ge NW by switching reaction gases to CH_4 and H_2. The optimized reaction conditions are a reaction time of 2 h at 870 °C. After the formation of Gr/Ge NWs, the morphologies were retained without structural damage (Figure 1c). The successful formation of graphene was confirmed by HRTEM, which shows

[*] H. Kim, C. Park, Prof. Dr. H. C. Choi
Department of Chemistry and
Division of Advanced Materials Science
Pohang University of Science and Technology
San 31, Hyoja-Dong, Nam-Gu, Pohang 790-784 (Korea)
E-mail: choihc@postech.edu
Homepage: http://www.postech.ac.kr/chem/nmrl
Y. Son, Prof. Dr. J. Cho
Interdisciplinary School of Green Energy
Ulsan National Institute of Science and
Technology (UNIST), Ulsan, 689-798 (South Korea)
E-mail: jpcho@unist.ac.kr
Homepage: http://jpcho.com

[**] This work was supported by the National Research Foundation of Korea (NRF) grant funded by MEST (grant numbers 2012-003040, 2012-053500, 2012-0009599, and 2010-00285), KOSEF through EPB center (grant number 2012-00000526), and ITRC by the MKE Korea (grant number 1415123286). The authors thank Hyun Jin Park in NCNT for his technical assistance in TEM analysis.

Supporting information for this article is available on the WWW under http://dx.doi.org/10.1002/anie.201300896.

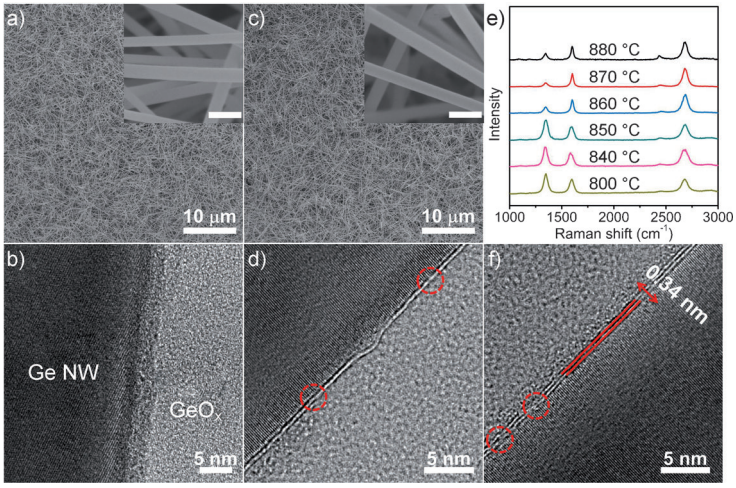

Figure 1. a and b) SEM and TEM images of as-grown Ge NWs, respectively. c and d) SEM and TEM images of Ge NW after the growth of graphene at 870 °C, respectively. The TEM image shows the formation of a single layer of graphene on a Ge NW. e) Raman spectra of a Gr/Ge NW grown at various temperatures. All spectra are normalized to the G peak intensities. f) Representative TEM image showing a bilayer of graphene grown on a Ge NW. The scale bars of the insets in (a) and (c) are 200 nm.

a Ge NW covered by a single layer of graphene (Figure 1 d). The Ge NW covered by a bilayer of graphene is also observed in Figure 1 f. The interlayer distance of the bilayer graphene is about 0.34 nm, which agrees well with the c-axis spacing of graphite. Most of the Gr/Ge NWs including the ones displayed at the dotted circles in both Figure 1 d and f show a high surface graphene coverage of the Ge NWs and apparent disconnection points along the growth axis. The presence of such defects helps the efficient access for Li ions to diffuse in and out of the Ge NWs (see below).

The presence of graphene and the degree of the defect level were further confirmed by Raman spectroscopy examining the intensities of the D, G, and G′ peaks as well as the ratios among the peaks. The appearance of both G and G′ peaks observed from the samples grown at temperatures ranging from 800 to 880 °C signifies that graphene is readily formed on Ge NWs by the metal-free CVD process. However, the quality of graphene determined by the intensity of the D peak (1346 cm^{-1}) corresponding to structural disorder[14] is highly dependent on the growth temperature (Figure 1 e). The intensity of the D peak basically decreases as the growth temperature increases, and the lowest intensity of the D peak with a I_D/I_G ratio of 0.50 is observed when the growth temperature is 870 °C (red graph in Figure 1 e), above which it increases again because of the deformation of the Ge NW prohibiting the smooth graphitization. Note that the Ge NW starts to melt at a temperature below 937 °C because of a size effect although the melting point of bulk Ge is at 937 °C.[15] Indeed, serious morphological destruction of the Ge NWs is observed when graphene growth is attempted at temperatures higher than 900 °C (Figure S1 in the Supporting Information).

Raman spectroscopy also provides information about the number of graphene layers on the Ge NWs from the I_G'/I_G ratio together with the full-width-at-half-maximum (FWHM) of the G' peak.[16] For the Gr/Ge NW grown at 870 °C, the I_G'/I_G is larger than 1 and the FWHM of the G' peak appearing at 2683 cm^{-1} is about 53 cm^{-1}. Each value is quite off from the one observed from the single layer of graphene grown on the Cu catalyst surface by CVD, which shows $I_G'/I_G \geq 2$ with a FWMH < 30–40 cm^{-1}.[17] This result indicates that the Gr/Ge NW is populated by a single or a few layers of graphene as also confirmed by TEM studies.[18] The low I_G'/I_G ratio originates from a non-negligible structural disorder that induces the breakage of the hexagonal symmetry in graphene, resulting in a decrease of the symmetry-allowed G′ peak intensity.[19] The homogeneity and elemental confirmation of graphene on the Ge NWs was achieved by electron energy loss spectroscopy (EELS) mapping under TEM conditions, which shows the presence of distinct C and Ge atoms on the surface and core of the Gr/Ge NW, respectively (Figure S2).

A possible involvement of the Au catalyst present at the tip of Ge NW for the growth of graphene was excluded by confirming the unabated successful growth of graphene on a Au-free Ge NW (Figure S3). The successful formation of Gr/Ge NW by the CVD method without using a conventional metal catalyst, such as Cu and Ni, resembles the successful growth of large-size single-layer graphene and single-layer graphene pads on α-Al_2O_3[20] and h-BN[21] substrates, respectively, under the same reaction conditions. The latter two cases demonstrate that the nucleation and propagation of graphitization succeeds as long as the substrate surface provides a highly ordered flatness, and a as-grown Ge NW seems to be flat enough to accommodate carbonaceous species to be nucleated. Note that most of the native GeO_x layer clearly visible in Figure 1 b is significantly reduced after growing graphene on a Ge NW (Figure 1 d and f), probably because of the presence of H_2 gas during the CVD process. Furthermore, the binary phase diagram of C and Ge is quite similar to that of C and Cu, according to which formation of solid solutions of C-Ge and C-Cu is quite difficult.[22] This implies that graphene is formed on a Ge NW preferably by adsorption of C on a Ge NW followed by nucleation and propagation into graphene rather than by following the precipitation mechanism applied for some transition-metal catalysts.[23]

The Gr/Ge NW containing a single to a few layers of graphene with appropriate amounts of defects is an ideal system for both allowing facile access of Li ions into and out of the Ge NW as well as protecting the Ge NW from its volume expansion. Having a few layers of graphene is especially critical for the facile access of Li ions as Li ions cannot diffuse in perpendicular direction to the pure basal plane of graphene, while Li ions travel through defects, such as vacancies and the grain boundary.[24] Recently, Yao et al. have claimed that six graphitic layers are a critical thickness for Li ions to diffuse in perpendicular direction to the basal plane of graphene regardless of the defect population.[24d]

To evaluate the Gr/Ge NW as an anode for the Li ion battery, the Gr/Ge NW was fabricated into Li half-cells (2016R type) and its performance was examined under various cell conditions below 24 °C. The successful lithia-

tion–delithiation occurring at the Gr/Ge NW was first investigated by electrochemical cyclic voltammetry using Li as a reference electrode (Figure S4). Then, all the fabricated half-cells were charged (alloying) and discharged (dealloying) at 0.05 C during the first cycle to form a smooth solid electrolyte interphase (SEI) on the surface of the electrode,[25] and the cells were charged and discharged at designated C-rates from the second cycle. Figure 2a shows voltage profiles between 0.001 and 1.5 V at 4.0 C. After the first charging, the measured specific capacity is higher than the theoretical capacity value (1600 mA h g^{-1}) with a coulombic efficiency of 69%, which owes to the SEI formed during the first charging step (Figure 2b).[5] Beyond the second charging/discharging cycle, the Gr/Ge NW shows a long cycle life and high specific capacity at 4.0 C. The specific capacity is 1059 mA h g^{-1} after 200 cycles with 90% of capacity retention that is defined as the change of specific capacity upon discharging from the 24th cycle at which the specific capacity reaches its maximum value. The coulombic efficiency starts to show a stable value ranging from 98.3 to 99.7% from the second cycle to the 200th cycle (Figure 2b), which indicates that the Gr/Ge NW has an excellent reversibility in charging and discharging by Li^+ ions once the SEI is formed.

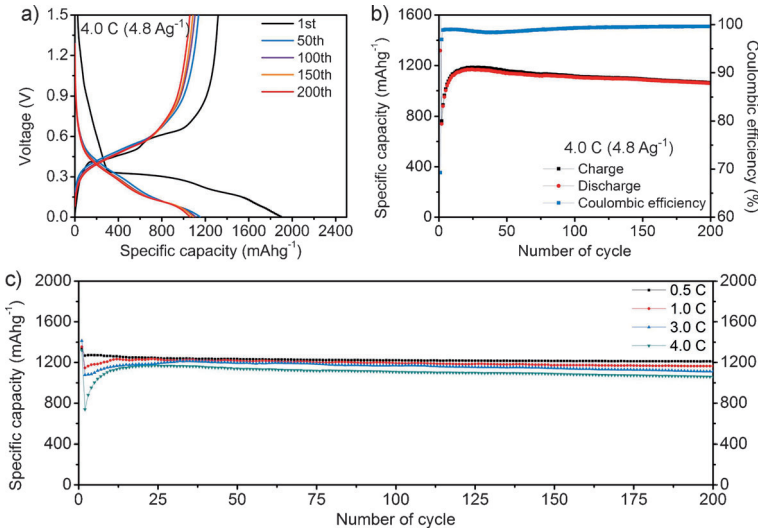

Figure 2. a) Voltage profiles of a Gr/Ge NW between 0.001 and 1.5 V at a rate of 4.0 C. b) Cycle performance of a Gr/Ge NW and coulombic efficiency at a rate of 4.0 C. c) Cycle performance of a Gr/Ge NW at each C-rate from 0.5 to 4.0 C (discharge). In the first cycle, the half-cell was charged and discharged at a rate of 0.05 C.

The trend in capacity retention was monitored at various C-rates, such as 0.5, 1.0, 3.0 and 4.0 C. As shown in Figure 2c, the capacity retention is well retained for various charging/discharging rates up to 4.0 C without significant drop of the specific capacity. For example, the specific capacities measured after 200 cycles at 0.5 and 4.0 C are 1210 and 1059 mA h g^{-1}, respectively. The capacity retentions after 200 cycles at 0.5 and 4.0 C are 95 and 90%, respectively (Figure 2c). Especially the specific capacity measured after 400 cycles at 0.5 C is 1176 mA h g^{-1} with capacity retention of 92% (Figure S5). Note that the contribution of graphene itself to the measured specific capacity is negligible considering that the weight percentage of graphene is only about 1.7%.

Such a long cycle life with a high specific capacity even at a high C-rate is remarkable as the performance of the Gr/Ge NW well exceeds the previously reported Ge systems coated either with amorphous carbon or RGO.[6,7,8,26,27] Considering that most of the degradation of the Ge anode involves destruction of the Ge structure because of the volume expansion during the charging process, the long cycle life with high capacity retention realized from the Gr/Ge NW seems to be attributed to intimate contact between graphene and the Ge NW as graphene holds the Ge NW tightly to accommodate the mechanical strain effectively. Moreover, the high electrical conductivity of graphene at a relatively low defect level is beneficial for the overall electron communication during the cycles. It is quite remarkable that the mechanical strain of the Ge NW is effectively suppressed only by a couple of graphene layer. As a control experiment, we performed test experiments with bare Ge NWs at 4.0 C. As shown in Figure 3a, the bare Ge NW exhibits much lower specific capacity (321 mA h g^{-1}) after 200 cycles and poor capacity retention of 41%. Figure S6a shows the corresponding voltage profiles of a Ge NW at 4.0 C. Note that the same data for the Gr/Ge NW shown in Figure 2b was reused for a direct comparison. The rate capabilities measured for both the bare Ge NW and the Gr/Ge NW from 0.2 to 20 C also support the efficient

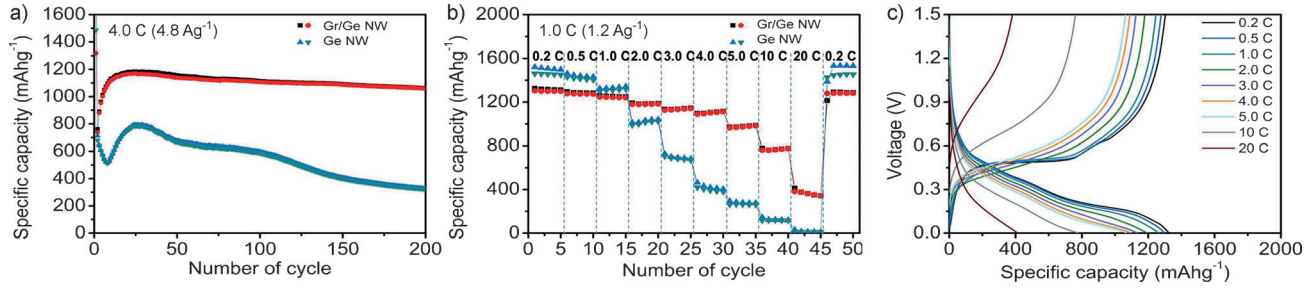

Figure 3. a) Comparison of the cycle performance of a Gr/Ge NW and a bare Ge NW at a rate of 4.0 C. b) Rate capability of a Gr/Ge NW and a bare Ge NW from 0.2 to 20 C. Legends: blue ▲ charging of the Ge NW, green ▼ discharging of the Ge NW, black ■ charging of the Gr/Ge NW, and red ● discharging of the Gr/Ge NW. c) Voltage profiles of the Gr/Ge NW corresponding to the rate capability measurement in (b).

protection of the Ge NW by graphene. As previously mentioned, the Gr/Ge NW sample shows an excellent rate capability even at a high C-rate (Figure 3b, black for charging and red for discharging). For example, the specific capacity of the Gr/Ge NW is about 363 $mA\,h\,g^{-1}$ at 20 C ($=24\,A\,g^{-1}$), which is comparable to the theoretical specific capacity of graphite. Moreover, when the C-rate is returned to the initial 0.2 C after 45 cycles, the specific capacity is well recovered (98.6%). However, in the case of a bare Ge NW, the specific capacity reduces rapidly upon the increase in the C-rate from 0.2 to 20 C with a specific capacity of 20 $mA\,h\,g^{-1}$ at 20 C (Figure 3b, blue for charging and green for discharging). Note that the voltage profiles for the rate capability of the Gr/Ge NW and the bare Ge NW are shown in Figure 3c and Figure S6b, respectively.

The successful protection of the Ge NW by a graphene layer was also observed from SEM (Figure S7) and TEM images showing large population of Ge NWs still coated with a couple of layers of graphene after 200 cycles at 4.0 C (Figure 4 and Figure S8). On the other hand, in the case of a pure Ge NW, no Ge NW was found after running the cell

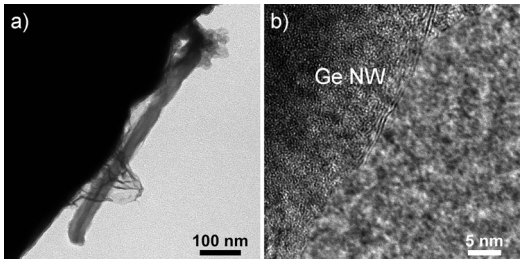

Figure 4. TEM images of the Gr/Ge NW after 200 cycles at 4.0 C. a) Low-magnification TEM image of a Gr/Ge NW. b) HR-TEM image of the Gr/Ge NW in (a), showing the graphene retained on the surface of the Ge NW.

under the same condition, which indicates that a Ge NW without graphene is quickly pulverized (Figure S9). Note that both samples were rinsed with acetonitrile and acetic acid before TEM measurements to remove the SEI layer.[28]

In summary, graphene grows directly on the surface of a Ge NW by a CVD process without any metal catalyst involved. The number of layers of graphene ranges from a single up to four layers, and the quality of graphene in terms of the defect level determined by Raman spectroscopy is comparable to that of graphene grown by a conventional metal-catalyzed process. The Gr/Ge NW shows a high performance as a Li ion battery anode as it exhibits a high specific capacity (1059 $mA\,h\,g^{-1}$) at a high C-rate (4.0 C) and a long cycle life (200 cycle) at a high capacity retention (90%). The performance of the Gr/Ge NW judged by these key parameters is superior to that of a bare Ge NW that is pulverized in a few charging/discharging cycles. The high performance of the Gr/Ge NW is attributed to the tight encapsulation of the Ge NW with high purity graphene. We believe that our findings will contribute not only to the fundamental understandings about the surface chemistry involved in the metal-catalyst-free growth of graphene by CVD on single crystalline nanowires, but also to the strategic developments of surface-protected materials with graphene.

Experimental Section

Synthesis of the Ge NW: The Ge NW was synthesized by a Au nanoparticle (NP)-assisted VLS process using liquid silicon tetrachloride ($SiCl_4$, 99.998%, Alfa Aesar) and germanium tetrachloride ($GeCl_4$, 99.9999%, Alfa Aesar) precursors. Both precursors were used without further purification. The Au catalyst was deposited on the Si(111) wafer by electroless deposition.[13] The successful formation of the Au NP was confirmed by atomic force microscopy (AFM) as it shows Au NPs with an average diameter of 20 nm (Figure S10). A Si wafer containing Au NPs was located at the center of a quartz tube, which was placed at the center of a tube furnace. The air trapped in the quartz tube was flushed out by argon (180 sccm) and hydrogen gas (30 sccm). After 10 minutes of flushing, the furnace was heated, and 2 sccm of $GeCl_4$ and 5 sccm of $SiCl_4$ both diluted with Ar were introduced at 760 °C for 1 h. Once the reaction was completed, the sample was cooled down by opening the cover of the furnace in H_2 environment.

Direct growth of graphene onto a germanium nanowire: A Si wafer piece containing Ge NWs was introduced into the same reactor used for growth of a Ge NW, and switching gases with 50 sccm of CH_4 and 50 sccm of H_2 at 870 °C for 2 h. After the reaction was completed, the sample was cooled down by opening the cover of the furnace in H_2 environment.

Characterization: The structure of the Ge and Gr/Ge NWs were characterized by scanning electron microscopy (SEM, JEOL, JSM-7410F), powder X-ray diffraction (XRD, RIGAKU, D/MAX-250/PC), transmission electron microscopy (TEM, JEOL, JEM-2200FS with image Cs-corrector) at the National Center for Nanomaterials Technology (NCNT) at POSTECH. A Raman spectrometer (WITEC Alpha 300R) equipped with a 532 nm diode laser below 2 mW of laser excitation power was used to characterize the quality and number of the layers of as-synthesized graphene on a Ge NW. The weight percentage of graphene in a Gr/Ge NW was characterized by elemental analysis (Thermo Scientific, Element Analyzer) at UNIST.

Electrochemical measurements: A slurry was made by mixing Gr/Ge NWs, ketjen black, polyacrylic acid (PAA), and carboxymethyl cellulose (CMC) in a weight ratio of 70:15:7.5:7.5. The bare Ge NW sample was fabricated by the same method as the Gr/Ge NW. The slurry was pasted on a Cu foil by the doctor-blade method. The half-cell was then assembled with a lithium foil (reference electrode), a polyethylene separator, and an electrolyte solution of 1.3 M $LiPF_6$ in ethylene carbonate/ethyl methyl carbonate (wt% 3:7) with 10% of fluoroethylene carbonate (Panax Starlyte). The loading amount of the slurry on the Cu foil ranged was from 1.0 to 1.9 $mg\,cm^{-2}$. The specific capacity was measured within a voltage window between 0.001 and 1.5 V at various C-rates. The specific capacity was calculated based on the mass of the active anode material (total mass of the Ge NW and graphene). Cyclic voltammetry was conducted at a scan rate of 0.1 $mV\,s^{-1}$.

Received: February 1, 2013
Revised: April 9, 2013
Published online: April 24, 2013

Keywords: graphene · lithium ion battery · nanowires · surface chemistry

[1] C. K. Chan, H. Peng, G. Liu, K. McIlwrath, X. F. Zhang, R. A. Huggins, Y. Cui, *Nat. Nanotechnol.* **2008**, *3*, 31–35.
[2] C. K. Chan, X. F. Zhang, Y. Cui, *Nano Lett.* **2008**, *8*, 307–309.

[3] M. Noh, Y. Kwon, H. Lee, J. Cho, Y. Kim, M. G. Kim, *Chem. Mater.* **2005**, *17*, 1926 – 1929.
[4] D. Wang, Y. L. Chang, Q. Wang, J. Cao, D. B. Farmer, R. G. Gordon, H. Dai, *J. Am. Chem. Soc.* **2004**, *126*, 11602 – 11611.
[5] J. Graetz, C. C. Ahn, R. Yazami, B. Fultz, *J. Electrochem. Soc.* **2004**, *151*, A698 – A702.
[6] A. M. Chockla, M. G. Panthani, V. C. Holmberg, C. M. Hessel, D. K. Reid, T. D. Bogart, J. T. Harris, C. B. Mullins, B. A. Korgel, *J. Phys. Chem. C* **2012**, *116*, 11917 – 11923.
[7] J. Cheng, J. Du, *CrystEngComm* **2012**, *14*, 397 – 400.
[8] D. J. Xue, S. Xin, Y. Yan, K. C. Jiang, Y. X. Yin, Y. G. Guo, L. J. Wan, *J. Am. Chem. Soc.* **2012**, *134*, 2512 – 2515.
[9] H. Wang, L. F. Cui, Y. Yang, H. S. Casalongue, J. T. Robinson, Y. Liang, Y. Cui, H. Dai, *J. Am. Chem. Soc.* **2010**, *132*, 13978 – 13980.
[10] Y. Wu, P. Yang, *Appl. Phys. Lett.* **2000**, *77*, 43 – 45.
[11] E. Sutter, P. Sutter, *Adv. Mater.* **2006**, *18*, 2583 – 2588.
[12] A. Pandurangan, C. Morin, D. Qian, R. Andrews, M. Crocker, *Carbon* **2009**, *47*, 1708 – 1714.
[13] H. J. Song, S. M. Yoon, H. J. Shin, H. Lim, C. Park, H. C. Choi, *Chem. Commun.* **2009**, 5124 – 5126.
[14] M. M. Lucchese, F. Stavale, E. H. M. Ferreira, C. Vilani, M. V. O. Moutinho, R. B. Capaz, C. A. Achete, A. Jorio, *Carbon* **2010**, *48*, 1592 – 1597.
[15] P. Buffat, J. P. Borel, *Phys. Rev. A* **1976**, *13*, 2287 – 2298.
[16] A. Gupta, G. Chen, P. Joshi, S. Tadigadapa, P. C. Eklund, *Nano Lett.* **2006**, *6*, 2667 – 2673.
[17] a) P. W. Sutter, J. I. Flege, E. A. Sutter, *Nat. Mater.* **2008**, *7*, 406 – 411; b) L. Gao, J. R. Guest, N. P. Guisinger, *Nano Lett.* **2010**, *10*, 3512 – 3516.
[18] D. S. Lee, C. Riedl, B. Krauss, K. von Klitzing, U. Starke, J. H. Smet, *Nano Lett.* **2008**, *8*, 4320 – 4325.
[19] A. C. Ferrari, *Solid State Commun.* **2007**, *143*, 47 – 57.
[20] H. J. Song, M. Son, C. Park, H. Lim, M. P. Levendorf, A. W. Tsen, J. Park, H. C. Choi, *Nanoscale* **2012**, *4*, 3050 – 3054.
[21] M. Son, H. Lim, M. Hong, H. C. Choi, *Nanoscale* **2011**, *3*, 3089 – 3093.
[22] R. I. Scace, G. A. Slack, *J. Chem. Phys.* **1959**, *30*, 1551 – 1555.
[23] X. Li, W. Cai, L. Colombo, R. S. Ruoff, *Nano Lett.* **2009**, *9*, 4268 – 4272.
[24] a) V. Meunier, J. Kephart, C. Roland, J. Bernholc, *Phys. Rev. Lett.* **2002**, *88*, 075506; b) C. Lee, B. Mun, P. N. Ross, *J. Electrochem. Soc.* **2002**, *149*, A1286 – A1292; c) T. Takamura, K. Endo, L. Fu, Y. Wu, K. J. Lee, T. Matsumoto, *Electrochim. Acta* **2007**, *53*, 1055 – 1061; d) F. Yao, F. Güneş, H. Q. Ta, S. M. Lee, S. J. Chae, K. Y. Sheem, C. S. Cojocaru, S. S. Xie, Y. H. Lee, *J. Am. Chem. Soc.* **2012**, *134*, 8646 – 8654.
[25] J. Shim, R. Kostecki, T. Richardson, X. Song, K. A. Striebel, *J. Power Sources* **2002**, *112*, 222 – 230.
[26] M. H. Seo, M. Park, K. T. Lee, K. Kim, J. Kim, J. Cho, *Energy Environ. Sci.* **2011**, *4*, 425 – 428.
[27] M. H. Park, Y. Cho, K. Kim, J. Kim, M. Liu, J. Cho, *Angew. Chem.* **2011**, *123*, 9821 – 9824; *Angew. Chem. Int. Ed.* **2011**, *50*, 9647 – 9650.
[28] J. W. Choi, J. McDonough, S. Jeong, J. S. Yoo, C. K. Chan, Y. Cui, *Nano Lett.* **2010**, *10*, 1409 – 1413.

